Liquid Crystals
Publication details, including instructions for authors and subscription information:
http://www.informaworld.com/smpp/title~content=t713926090

Chiral ordering in the nematic and an optically isotropic mesophase of bent-core mesogens with a halogen substituent at the central core

Wolfgang Weissflog[a]; Siegmar Sokolowski[b]; Heinz Dehne[b]; Banani Das[c]; Siegbert Grande[c]; Martin W. Schröder[a]; Alexey Eremin[a]; Siegmar Diele[a]; Gerhard Pelzl Corresponding author[a]; Horst Kresse[a]
[a] Institut für Physikalische Chemie, Martin-Luther-Universität Halle-Wittenberg, D-06108 Halle (Saale), Germany [b] Fachbereich Chemie, Universität Rostock, D-18055 Rostock, Germany [c] Institut für Experimentelle Physik I, Universität Leipzig, D-04103 Leipzig, Germany

Online publication date: 25 May 2010

To cite this Article Weissflog, Wolfgang , Sokolowski, Siegmar , Dehne, Heinz , Das, Banani , Grande, Siegbert , Schröder, Martin W. , Eremin, Alexey , Diele, Siegmar , Pelzl Corresponding author, Gerhard and Kresse, Horst(2004) 'Chiral ordering in the nematic and an optically isotropic mesophase of bent-core mesogens with a halogen substituent at the central core', Liquid Crystals, 31: 7, 923 — 933
To link to this Article: DOI: 10.1080/02678290410001704982
URL: http://dx.doi.org/10.1080/02678290410001704982

LIQUID CRYSTALS, VOL. 31, NO. 7, JULY 2004, 923–933

Chiral ordering in the nematic and an optically isotropic mesophase of bent-core mesogens with a halogen substituent at the central core

WOLFGANG WEISSFLOG, SIEGMAR SOKOLOWSKI†, HEINZ DEHNE†, BANANI DAS‡, SIEGBERT GRANDE‡, MARTIN W. SCHRÖDER, ALEXEY EREMIN, SIEGMAR DIELE, GERHARD PELZL* and HORST KRESSE

Institut für Physikalische Chemie, Martin-Luther-Universität Halle-Wittenberg, Mühlpforte 1, D-06108 Halle (Saale), Germany
†Fachbereich Chemie, Universität Rostock, Buchbinderstr. 9, D-18055 Rostock, Germany
‡Institut für Experimentelle Physik I, Universität Leipzig, Linnéstr. 5, D-04103 Leipzig, Germany

(*Received 14 November 2003; accepted 28 February 2004*)

Two new homologous series of bent-core compounds have been synthesized. Their mesophase behaviour has been investigated by polarizing microscopy, differential scanning calorimetry, X-ray diffraction, NMR spectroscopy, and by dielectric and electro-optical measurements. It was found that, with one exception, all the chlorine-substituted compounds form a nematic phase and an optically isotropic 'banana phase'. The latter phase shows spontaneously chiral domains of opposite handedness. This phase may be considered as a type of smectic blue phase. The mesophase behaviour of the homologous bromine-substituted compounds is more complicated. Depending on the chain length, B_6, columnar, nematic or the isotropic 'banana phase' occur.

1. Introduction

Recently we showed in a preliminary communication that 4-chlororesorcinol bis[4-(4-*n*-dodecyloxybenzoyloxy)benzoate] forms two mesophases with unusual properties. The high temperature phase is a nematic phase which spontaneously exhibits domains with opposite handedness and which shows a smectic-like fan-shaped texture on application of a sufficiently high electric field. The low temperature phase is a highly viscous optically isotropic phase which forms chiral domains of opposite handedness. X-ray investigations provided evidence that this phase possesses a periodicity with reduced long range order [1]. Thus the usual cubic phase is ruled out. In order to study this unusual behaviour in more detail we have synthesized other homologue belonging to the same series and, in addition, 10 analogous bromine-substituted homologues see figure 1.

The phase behaviour of all these new compounds has been investigated by polarizing optical microscopy, differential scanning calorimetry, X-ray diffraction, NMR spectroscopy and by dielectric and electro-optical measurements.

*Author for correspondence;
e-mail: pelzl@chemie.uni-halle.de

2. Materials

The compounds were prepared by the reaction of 4-chlororesorcinol or 4-bromoresorcinol with the corresponding 4-(4-*n*-alkyloxybenzoyloxy)benzoic acids, using dicyclohexylcarbodiimide according to the method already described for 4-chloro-1,3-phenylene bis[4-(4-*n*-dodecyloxybenzoyloxybenzoate] [1]. Their thermal properties are given in table 1.

3. Experimental

The thermal behaviour of the compounds (transition temperatures, and associated transition enthalpies) was investigated using a differential scanning calorimeter (Pyris 1, Perkin-Elmer). The microscopic textures and the field-induced texture changes were examined using a polarizing microscope (Leitz Orthoplan) equipped with a Linkam hot stage (TMS 91).

X-ray investigations on non-oriented samples were

Liquid Crystals ISSN 0267-8292 print/ISSN 1366-5855 online © 2004 Taylor & Francis Ltd
http://www.tandf.co.uk/journals
DOI: 10.1080/02678290410001704982

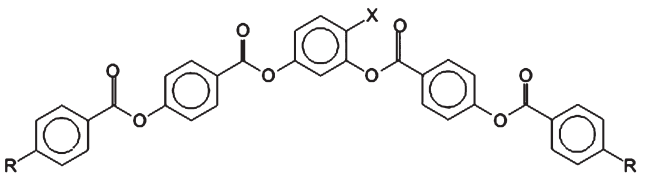

Figure 1. Chemical structure of the investigated compounds (X = Cl, Br; R = alkyloxy, alkyl).

performed using the Guinier method. Oriented samples were obtained by applying a magnetic field of about 1 T. The patterns were recorded using a flat-film camera and/or using a two-dimensional detector (HI-STAR Area Detector, Siemens AG). The Ni-filtered Cu-K_α radiation was collimated by a pinhole with a diameter of 0.3 mm. The profile of the small angle scattering corresponding to the length of the molecules was measured with a small angle camera (Kratky principle). The correlation length ξ was estimated via $\xi = 2/\Delta q$ using the full width at half maximum (FWHM).

Dielectric measurements were carried out in the frequency range 1 Hz to 10 MHz using a Solartron-Schlumberger Impedance Analyzer S 1260 and a Chelsea Interface. A double plate cell ($d = 0.1$ mm) made from brass and coated with gold was used as capacitor. Cyclohexane was used for calibration. The sample was oriented by a magnetic field of 0.6 T. Electro-optical investigations were performed using the usual experimental set-up where the cells (E.H.C. Corp.) are heated on the hot stage of the polarizing microscope and a power supply (Keithley 3910) generates the voltage signals.

NMR measurements were made using a Bruker MSL 500 spectrometer at a field of 11.7 T. The temperature of the 5-mm sample tubes was regulated by a Bruker BST 100 temperature controller. The proton decoupled ^{13}C spectra at 125 MHz were recorded in the isotropic state using pulse excitation together with the WALTZ decoupling method. For the liquid crystalline phase, pulse and CP excitation were used for ^{13}C resonance and the spectra were observed using WALTZ and high power decoupling. The order parameter was estimated from the proton spectra obtained from ^{1}H NMR measurements and compared with those determined from ^{13}C NMR studies. The conformational aspects of

Table 1. Transition temperatures (°C) and associated enthalpy changes (kJ mol^{-1}) for the compounds studied, see figure 1.

Compound	R	X	Phase behaviour								
9Cl	OC_9H_{19}	Cl	Cr	86 [36.6]	(X	69) [5.3]	N	95 [0.5]	I		
10Cl	$OC_{10}H_{21}$	Cl	Cr	89 [62.5]	(X	65) [6.1]	N	96 [0.6]	I		
11Cl	$OC_{11}H_{23}$	Cl	Cr	88 [66]	(X	73) [8.6]	N	95 [0.6]	I		
12Cl	$OC_{12}H_{25}$	Cl	Cr	98 [38.7]	(X	80) [9.1]	N	95 [0.7]	I		ref. [1]
16Cl	$OC_{16}H_{33}$	Cl	Cr	99 [34.8]	(SmX	88 [3.5]	N	92) [1.2]	I		ref. [2]
5'Br	C_5H_{11}	Br	Cr	108 [27.4]	(Col	63 [5.75]	N	74) [0.25]	I		
5Br	OC_5H_{11}	Br	Cr	110 [52.8]	(B_6	109) [8.1]			I		
6Br	OC_6H_{13}	Br	Cr	119.5 [54.3]	(B_6	101.5) [–]			I		
7Br	OC_7H_{15}	Br	Cr	93.5 [47.4]	(B_6	87 [5.9]	N	93) [0.5]	I		
8Br	OC_8H_{17}	Br	Cr	94 [41.1]	(Col	75 [5.4]	N	90) [1.9]	I		
9Br	OC_9H_{19}	Br	Cr	88 [24.3]			(N	83) [0.5]	I		
10Br	$OC_{10}H_{21}$	Br	Cr	87 [60.4]	(Cr I	66 [24.9]	N	87) [0.5]	I		
11Br	$OC_{11}H_{23}$	Br	Cr	87.5 [73.4]	(Cr I	72 [19.7]	N	82) [0.5]	I		
12Br	$OC_{12}H_{25}$	Br	Cr	92 [63.4]	(X	78 [13.7]	N	86.5) [0.5]	I		
14Br	$OC_{14}H_{29}$	Br	Cr	93 [29.7]	(X	83 [9.0]	N	86) [0.4]	I		

the molecule under study were determined mainly from the ^{13}C NMR measurements.

4. Results

4.1. *Chlorine-substituted compounds*

4.1.1. *Optical and electro-optical investigations*

As seen in table 1, all the chlorine-substituted homologues exhibit a nematic phase. The homologues **9Cl**–**12Cl** form, in addition, an isotropic mesophase preliminary designated as X. The optical isotropy could be clearly detected by refractometric studies. The hexadecyloxy compound **16Cl** has been described elsewhere [2]; it forms a smectic phase, designated as SmX. As shown for compound **12Cl**, the nematic phase displays some unusual properties. Over the whole temperature range of the nematic phase chiral domains of opposite handedness can be observed although the molecules are achiral. These domains can be seen by rotating one polarizer by a small angle from the crossed position or by illuminating the sample with circularly polarized light in the reflection mode of the microscope [1]. These domains are not uniform and fixed, however, and can be changed by mechanical stress or by temperature changes. The spontaneous formation of chiral domains is obviously the result of bend–twist deformations which are promoted by the bent shape of the molecules as seen elsewhere [3]. The occurrence of spontaneous twisted regions in nematic phases is also seen in computer simulations of bent molecules [4].

The nematic phase shows an unusual electro-optical response. If a d.c. field or low frequency field is applied to a planar oriented nematic phase, initially a domain pattern with equidistant stripes parallel to the original director direction is seen. With increasing voltage, the long wave nematic director fluctuations become weaker and initially a myeline-like texture and finally a fan-shaped texture is produced, which is reminiscent of a smectic phase. The field-induced textures disappear if the field is removed. Figure 2 shows (*a*) the field-induced myeline texture as well as (*b*) the fan-like texture in the nematic phase of compound **9Cl**. Figure 3 shows the nematic phase of compound **10Cl**; in the lower right section a d.c. field of 100 V is applied, while in the upper left section the field is absent. It can be seen that a smectic-like texture is generated by the electric field.

Another remarkable observation is the existence of a monotropic optically isotropic mesophase preliminarily designated as X which is formed on cooling the nematic

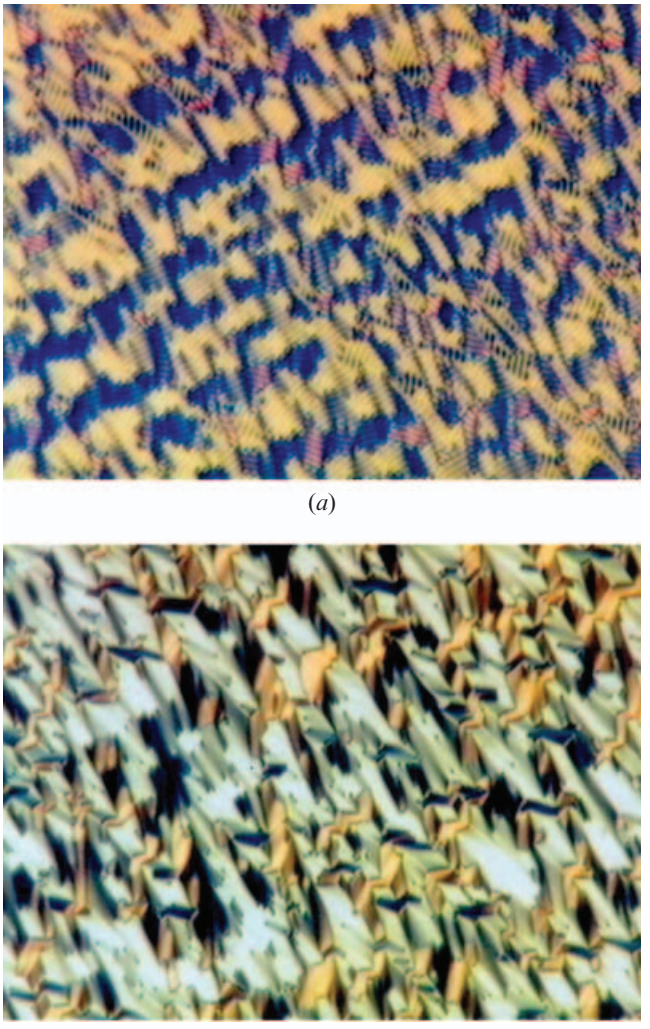

(*a*)

(*b*)

Figure 2. Field-induced texture of the nematic phase of compound **9Cl**: (*a*) 10 V, (*b*) 18 V (sample thickness 6 μm, temperature 92°C).

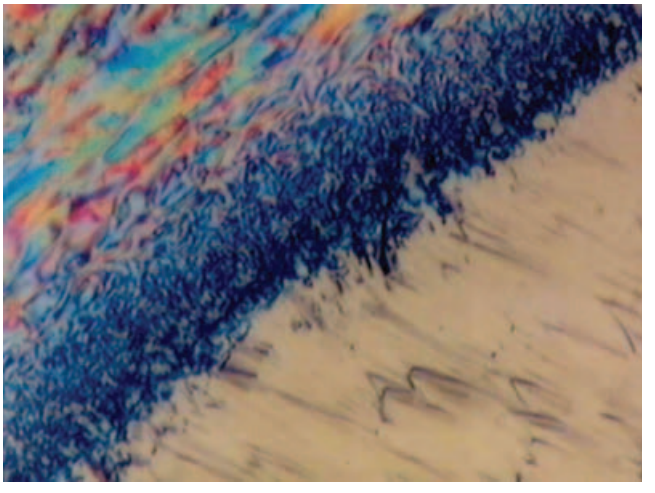

Figure 3. Optical texture of the nematic phase of compound **10Cl** (sample thickness 6 μm, temperature 91°C). In the lower right section an electric field of 16 V μm^{-1} is applied; in the upper left section the electric field is absent.

phase of the compounds **9Cl** to **12Cl**. This phase shows extinction between crossed polarizers. It spontaneously forms chiral domains of opposite handedness which are visible on rotating one polarizer by a small angle from the crossed position, see figures 4 (*a*) and 4 (*b*). These chiral domains are much more pronounced if the X phase is formed in the presence of a d.c. field.

4.1.2. *X-ray diffraction*

The X-ray pattern of well aligned samples in the nematic phase consists of a diffuse dumb-bell-like scattering maximum in the small angle region, and a diffuse wide angle scattering located around the equator, see figures 5 (*a*) and 5 (*c*). This is due to the existence of cybotactic smectic groups in the nematic phase. The molecules are tilted with respect to the layer normal. The tilt angle α was measured to be 48°.

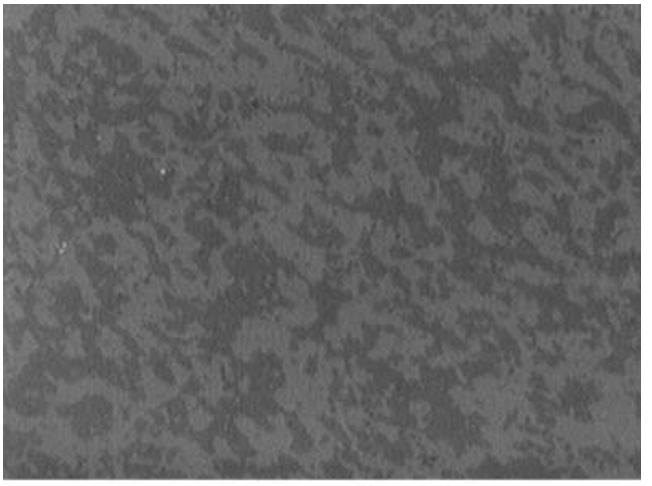

(*a*)

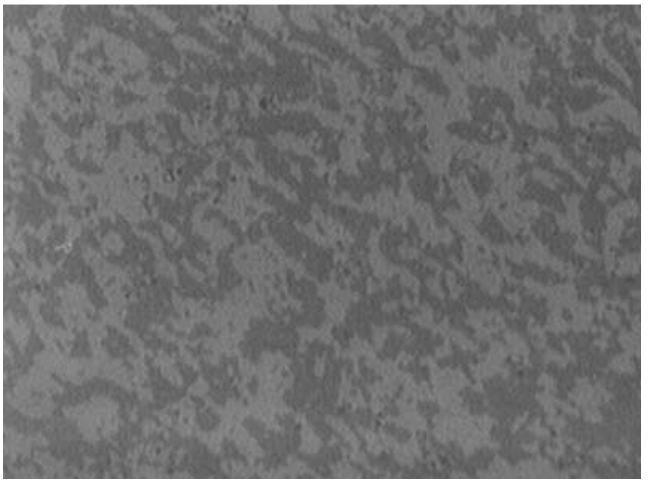

(*b*)

Figure 4. Chiral domains of opposite handedness in the X phase of compound **12Cl** seen by rotating one polarizer by 10° from the crossed position: (*a*) clock-wise, (*b*) anticlock-wise (sample thickness 10 μm, temperature 77°C).

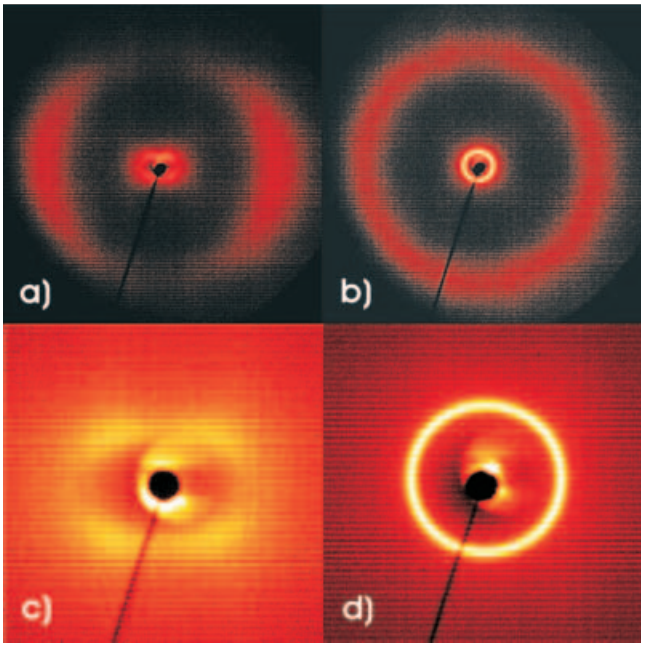

Figure 5. X-ray patterns of compound **12Cl** in the N phase (*a*) and the enlarged small angle region (*c*) as well as the corresponding patterns in the X phase (*b*) and (*d*).

At the transition from the nematic to the X phase, the diffuse spots in the small angle region are smeared to form a closed ring and the FWHM of the ring strongly decreases, see figures 5 (*b*) and 5 (*d*). This closed ring was obtained for each measurement, on repeating measurements, and for measurements of the different compounds. The outer diffuse scattering also forms a closed circle. It is worth mentioning that on cooling, the pattern of the crystalline phase again exhibits a strong preferred direction.

Figure 6 shows the scattering profiles of the small angle reflections in the nematic phase, X phase and, for a comparison, in the solid phase. As mentioned before, the FWHM in the X phase decreases but does not reach the instrumental resolution as expected for a smectic phase. This indicates that the X-phase has a layer structure but with a reduced correlation length. The correlation length has been calculated to be $\xi = 1.5$ nm in the nematic phase and $\xi = 11$ nm in the X phase. The layer normals can adopt arbitrary directions in space. The thickness of the layer ($d = 3.75$ nm) is considerably smaller than the length of the molecule ($L = 6$ nm, measured as the end to end distance of the bent molecule).

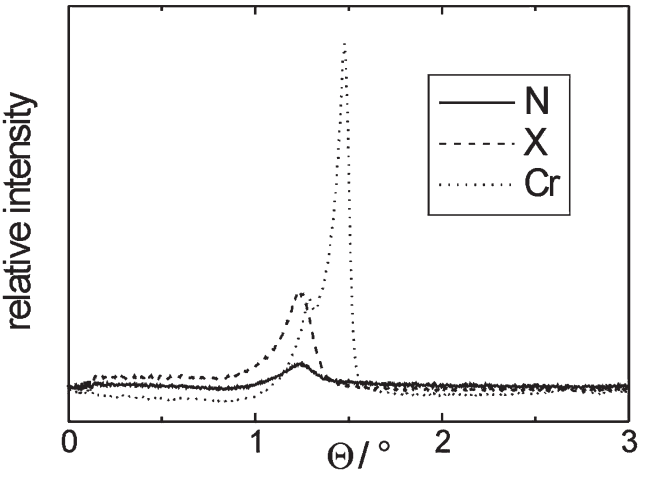

Figure 6. Scattering profiles in the nematic phase, X phase and crystalline phase of compound **12Cl**. For reasons of clarity the experimental scattering diagrams have been modified by division of the values in the isotropic phase.

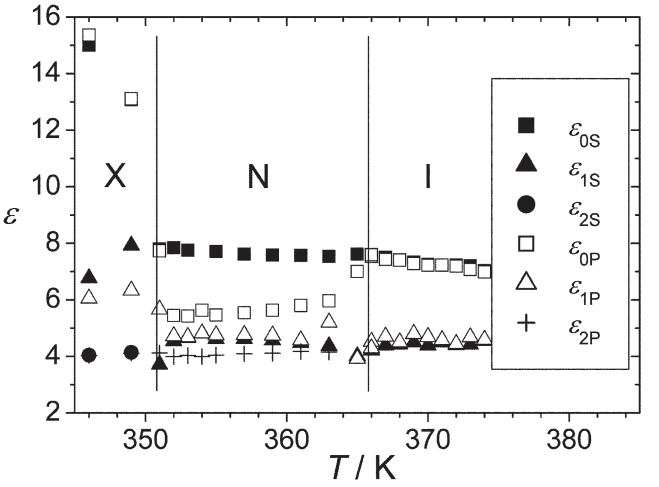

Figure 7. Dielectric permittivities in the isotropic, nematic and X phases of compound **12Cl**. The suffixes 0, 1 and 2 correspond to the limits of the dielectric permittivities. The suffixes P and S indicate dielectric permittivities parallel and perpendicular to, respectively, the director in the nematic phase.

4.1.3. *Dielectric measurements*

Dielectric measurements were performed on compound **12Cl** in a magnetic field of 0.6 T. The complex dielectric function $\varepsilon^*(f)=\varepsilon'(f)-i\varepsilon''(f)$ was fitted to equation (1) consisting of two Cole–Cole mechanisms (terms 1–3), a conductivity contribution (term 4) and term 5 for the description of the capacitance of the double layer at low frequencies:

$$\varepsilon*(f)=\varepsilon_2+\frac{\varepsilon_0-\varepsilon_1}{1+(i\omega\tau_1)^{1-\alpha_1}}+\frac{\varepsilon_1-\varepsilon_2}{1+(i\omega\tau_2)^{1-\alpha_2}}-\frac{iA}{f^M}+\frac{B}{f^N} \quad (1)$$

where ε_i are the low and high frequency limits of the dielectric permittivity, $\omega=2\pi f$ (f is the frequency), τ_i are relaxation times, α_i are Cole–Cole distribution parameters. A is the conductivity term which is related to the specific conductivity by $\kappa=2A\pi\varepsilon_0$ ($\varepsilon_0=8.85\times10^{-12}\,\mathrm{A\,s\,V^{-1}\,m^{-1}}$) if $N=1$, and M, B and N are further fit parameters responsible for the slope of conductivity and capacity of the double layer. The dielectric constants parallel (P) and perpendicular (S) to the nematic director are shown in figure 7. These symbols were extended to the X phase.

In the isotropic phase only one relaxation process is seen in the investigated frequency range which reduces the dielectric constant from about $\varepsilon_0=7$ to $\varepsilon_1=4$. In the nematic phase the dielectric properties become anisotropic. It is seen that the static dielectric anisotropy is negative ($\Delta\varepsilon=\varepsilon_{0P}-\varepsilon_{0S}<0$). Due to stronger hindrance of the reorientation about the short molecular axes, $\varepsilon_P^*(f)$ can be separated into two processes with the low frequency limits ε_{P0} and ε_{P1}, respectively. The related relaxation times τ_{1P} and τ_{2P} produced by the reorientation about the short and long axes of the molecules are presented in figure 8. In the perpendicular direction only a high frequency process is seen whose time constant agrees well with that of τ_{2P}. This dielectric behaviour is in accord with that of 'classical' nematic samples as described by Maier and Meier [5].

At the transition to the X phase a considerable increase of the static dielectric constant ε_0 is clearly seen indicating the positive dipole correlation. It is also found that the dielectric properties are isotropic, which means that there is no difference between the parallel and perpendicular directions. It is seen from figure 7, that in the X phase, ε_0 and ε_2 for the two main

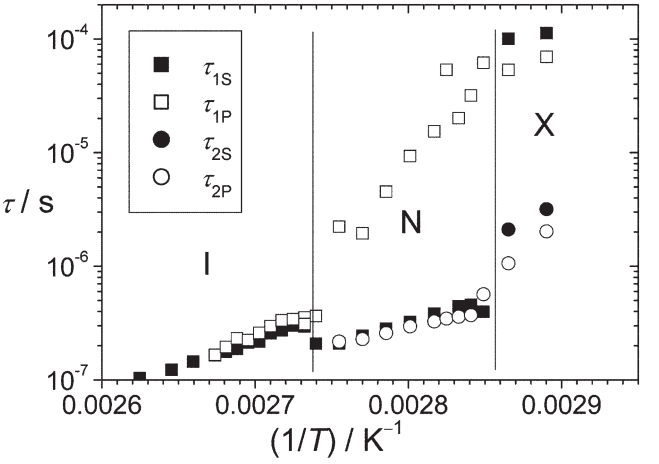

Figure 8. Temperature dependence of the relaxation times τ_1 and τ_2 in the isotropic, nematic and X phase of compound **12Cl**. The suffixes P and S correspond to the directions parallel and perpendicular to the director, respectively.

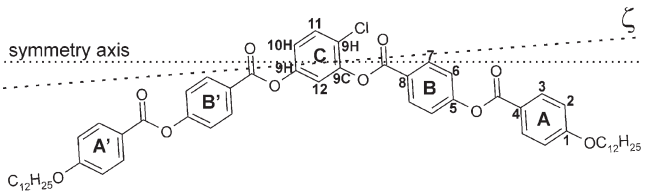

Figure 9. Sketch of the molecules and assignment of the atoms and rings for compound **12Cl**.

directions (P, S), which are directly measured, are identical. The errors in the ε_1 values indicated by full and open triangles are of the order of 20% since the broad relaxation range was divided into two relaxations by computer analysis. Furthermore it follows from figure 8 that the relaxation times τ_P and τ_S are also identical within the errors associated with the separation into the two mechanisms.

The relaxation times of the slower process in the X phase seem to continue that of the nematic phase. Therefore this mechanism may be caused by the reorientation of the molecules about their short axes. The increase of the relaxation time of the fast process at the transition N–X probably results from the stronger hindrance to reorientation about the long axis of the molecules. This process is connected with an increasing dipole correlation. Both results may be explained by a formation of layers. In comparison with other phases formed by banana-shaped molecules the change in the dynamics at the N–X transition is relatively small, indicating a phase with a 'liquid-like' order as found in the nematic or SmA phases.

4.1.4. *NMR spectroscopy*

NMR measurements were performed in the isotropic, nematic and X phases of compound **12Cl.** The numbering of the positions for the atoms in the molecule used for the assignment is shown in figure 9.

In figure 9 the assumed symmetry axis of the molecule and the molecular long axis, ζ, is indicated. The latter may deviate from the symmetry axis by a few degrees [6–8]. The chosen molecular frame should coincide with the main frame of the ordering matrix. The local surroundings for the rings A and B on the right and left hand side are identical as manifested by identical isotropic carbon shifts. However, due to the non-symmetric chlorine substitution at position 10, in the isotropic phase we resolve all six lines originating from the carbons in the central ring C. The assignment of the lines in the isotropic phase is shown in figure 10.

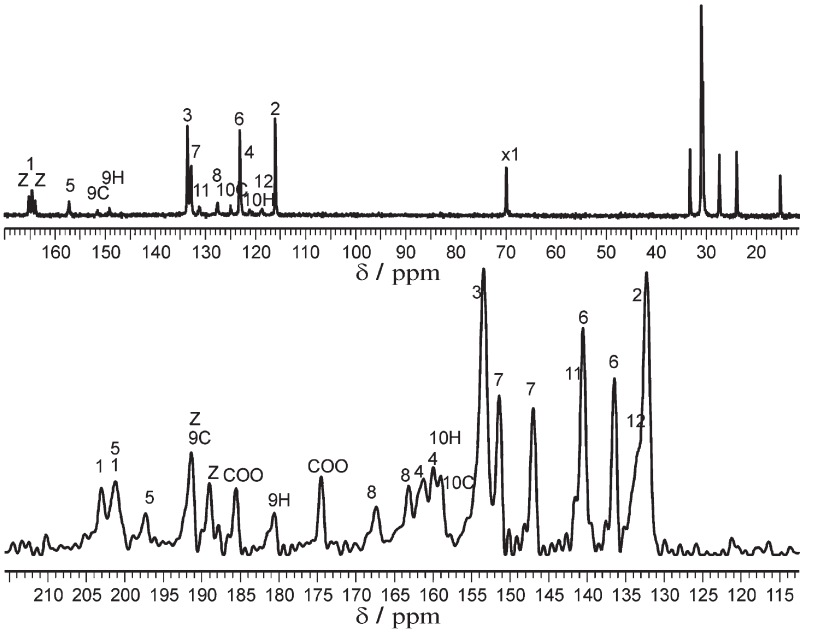

Figure 10. NMR spectra. Top: in the isotropic phase (105°C); bottom: in the nematic phase (87°C) of compound **12Cl**.

The transition into the nematic phase occurs within a range of 2 K. A small distribution of the director orientation gives an additional line broadening. The resolution in the spectra is further reduced by a strong overlap of lines in some regions. Similar to previous reports for banana-shaped mesogens with a non-symmetric cyano-substituted central core [7], the equivalence between the left and right legs are lost for the present molecules. Also, the substitution changes the shift tensors for all carbons of ring C in comparison with the values obtained for the symmetric rings [6, 9]. Using the line behaviour under different experimental conditions we propose the line assignment as shown in figure 10.

We consider the central ring as the stable part of the molecule and define the order parameters of this segment as the order of the whole molecule. The observed anisotropic shifts δ^{Ci} depend on the orientational order (S, D), see equation (2):

$$\delta^{\mathrm{C}i}_{\mathrm{obs}} = \delta^{\mathrm{C}i}_{\mathrm{iso}} + S\delta^{\mathrm{C}i}_{\zeta\zeta} + \frac{D}{3}\left(\delta^{\mathrm{C}i}_{\xi\xi} - \delta^{\mathrm{C}i}_{\eta\eta}\right) \qquad (2)$$

where $\delta^{\mathrm{C}i}_{\alpha\alpha}$ are the components of the shift tensors of the Ci-th carbon in the molecular main frame ξ, η, ζ, where ζ corresponds to the molecular long axis. The $\delta^{\mathrm{C}i}_{\xi\xi}$ depend on the orientation and magnitude of the main frame shift tensors $\delta^{\mathrm{C}i}_{ii}$. They are not known with the required precision for the calculation of S and D from four positions (9C, 9H, 10C and 10H) of the stable central ring. Therefore the contribution from the anisotropic order fluctuation, D, is neglected (first results from molecules with a deuterated central ring give D values of the order of 0.05 as shown in figure 11). We use values of $\delta^{9\mathrm{C}}_{\zeta\zeta} = 72$ ppm, $\delta^{9\mathrm{H}}_{\zeta\zeta} = 57.2$ ppm, $\delta^{10\mathrm{C}}_{\zeta\zeta} = 60.3$ ppm, $\delta^{10\mathrm{H}}_{\zeta\zeta} = 69.7$ ppm, similar to earlier investigated systems [8] for the calculation of S.

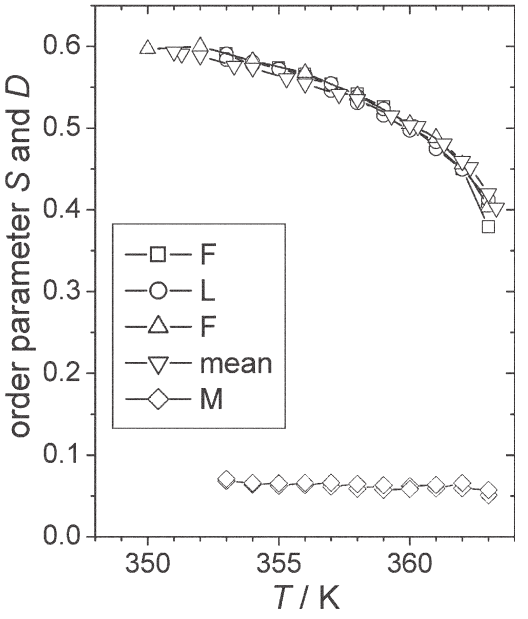

Figure 11. Temperature dependence of the order parameters S and D in the nematic phase of compound **12Cl**.

The temperature dependence of the averaged order parameter S is shown in figure 11. Within the nematic phase, S increases markedly from 0.39 at the clearing point to a value of 0.60 at the transition to the low temperature X phase.

The ^{1}H spectra consist of a well resolved line pair on a broader background from the protons of the chains. The aromatic proton pairs in all rings are relatively isolated and form angles of about 30° with the long axis. The observed line pair is an overlap of these three dipolar splittings. We assign the inner lines of an indicated fine structure to the proton pairs of ring C and get agreement of S (H NMR) with S (^{13}C NMR) for an angle of 3° between the symmetry axis and the long axis. Although the choice of the geometry is to a certain extent arbitrary, we cannot vary it by more than 2°.

The calculated values $S(T)$ are now used to obtain $\delta^i_{\zeta\zeta}$ for all the carbons in the two legs. The $\delta^i_{\zeta\zeta}$(s) are connected to the main frame shift tensors (δ^i_{11} and δ^i_{22}), by the relation:

$$\delta^i_{\zeta\zeta} = \langle \delta^{\mathrm{ip}}_{11} - \left(\delta^{\mathrm{ip}}_{11} - \delta^{\mathrm{ip}}_{22}\right)\sin^2\varepsilon - \left(\delta^{\mathrm{ip}}_{11} + 2\delta^{\mathrm{ip}}_{22}\right)\sin^2\varepsilon\sin^2\varphi\rangle. \quad (3)$$

The angle ε corresponds to the angle between the molecular long axis and the *para*-axis of the aromatic rings A or B, and φ describes the torsion of the ring planes A or B with respect to the plane of ring C (ξ, n plane). From ε, the bending angle $\alpha = 180° - 2\varepsilon$ can be determined.

The knowledge of the main frame components δ^i_{11} and δ^i_{22} for each position i of the rings A and B allows the evaluation of the time averaged geometries only, if the angles ε and φ are not correlated. Since the δ^i_{11} and δ^i_{22} values are not exactly known from single crystal investigations, we used values for δ^i_{11} derived from simple linear liquid crystalline reference compounds with the same substituents, and for δ^i_{22} typical values from the literature. The application of equation (2) for two positions in each ring leads to the angles given in table 2.

The angles of the rings A, A′ are found to be independent of temperature indicating that the

Table 2. The angles ε and φ for the rings A and B.

Angle/°	Ring A	Ring A′	Ring B	Ring B′
ε	21.5	24.0	20.0	21.0
φ	41.5	44.5	51.5	75.0

averaged conformations of the outer parts of the legs remain unchanged throughout the nematic range of the mesophase. The differences in the geometry of the outer rings A and A′ are small and the torsion angles φ for the rings A and A′ are of the order of 45°. This may be the result of an averaging over different torsion angles φ approaching a nearly axial-symmetric tensor in the *para*-axis frame. Since the long axis is tilted with respect to the symmetry axis by 3°, for one leg (our proposal is the right side in figure 9 where the Cl is substituted) the angle between the fixed symmetry axis and the *para*-axis is smaller for the ring A (17°) and larger for the other leg A′ on the left side (27°). As can be seen from table 2, rings B and B′ have noticeably different torsion angles with differences of the order of 20°. The effect of the non-symmetric chlorine substitution results in a stronger torsion of the COO plane on the right leg (of the order of 90°) due to the steric interaction with the Cl. This explains the larger torsion angle of ring B.

The bending angle ($180°-\varepsilon_A-\varepsilon'_A$) has been estimated for this molecule to be around 138° which is larger than that of conventional banana phases. This large bending angle may promote the formation of the nematic phase. However, it should be pointed out that from NMR studies we find this phase to behave as a normal nematic phase, although electro-optical studies indicate some unusual properties. It is likely that the pitch of the helix was large enough to be unwound in the presence of the strong external magnetic field of 11.7 T.

With regard to the low temperature X phase, our NMR results generally support the experimental observations from X-ray and optical studies [1] that the phase behaves isotropically. The NMR spectra show broad overlapping lines but with their centres at the positions of the isotropic chemical shifts as shown in figure 12. The time-averaged orientation of the molecules is isotropic. The different allowed directions of the molecular long axis must form a cubic arrangement. The time for the reorientation is longer than our measuring time of 10 ms suggesting either large distances between the directions or a low diffusion probability. This is obviously the reason that in the NMR spectra of the X phase the lines are broad and not sharp as in usual cubic phases. Since we only observe the average effect in NMR studies, the molecular motions may not be completely averaged within the time frame of NMR measurements and the phase probably has a 'pseudo-cubic' symmetry.

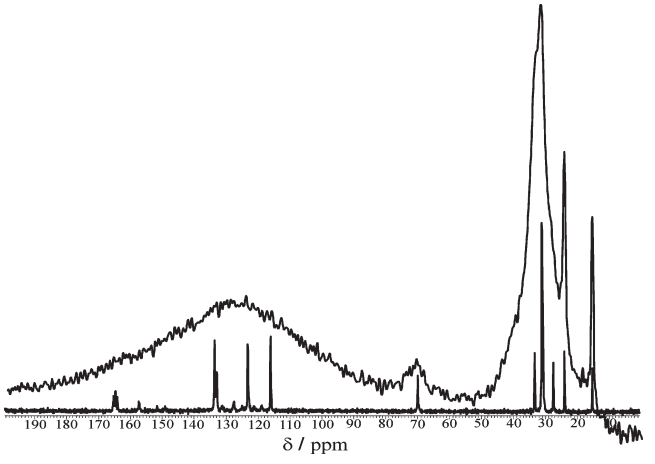

Figure 12. ^{13}C spectra in the isotropic (lower spectrum) and in the X phase (upper spectrum) of compound **12Cl**.

4.2. *Bromine-substituted compounds*

Despite the fact that additional phases appear in the Br-substituted compounds, the properties of the the nematic phase as well as the X phase are the same as reported for the Cl-substituted compounds. As seen from table 1 the homologues **7Br**–**14Br** exhibit a nematic phase which behaves quite similarly to that of the Cl-substituted compounds. Thus, the nematic phase spontaneously forms chiral domains of opposite handedness, see figure 13. Furthermore, on applying an electric field an unusual domain pattern can be observed. These domains, which are aligned perpendicular to the original director direction, contain equidistant stripes with a period of 40 μm, which is four times the sample thickness, see figure 14. At lower frequencies these domains are destroyed due to electro-hydrodynamical fluctuations. At higher d.c. fields smectic-like textures can be induced, as described for the Cl-substituted compounds.

Compound **9Br** does not exhibit a low temperature mesophase. The homologues **10Br** and **11Br** exhibit a weakly birefringent solid phase, whereas **12Br** and **14Br** form an isotropic mesophase on cooling the nematic phase. As shown for compound **12Br**, this highly viscous phase shows spontaneously chiral domains of opposite handedness (more pronounced in the presence of a d.c. field).

The X-ray patterns of well aligned samples again prove the existence of cybotactic groups in the nematic phase, see figure 15 (*a*). The tilt angle of the molecules within the cybotactic groups can be measured and was found to be 45°. The apparent length of the molecules in the cybotactic groups was estimated via the Bragg equation to be about 4.6 nm.

The transition to the X phase is again associated with the appearance of a closed ring in the small angle region connected with a decrease of the FWHM, see figure 15 (*b*). It is interesting that the mesophase behaviour of homologues with short terminal chains is different in comparison with the corresponding

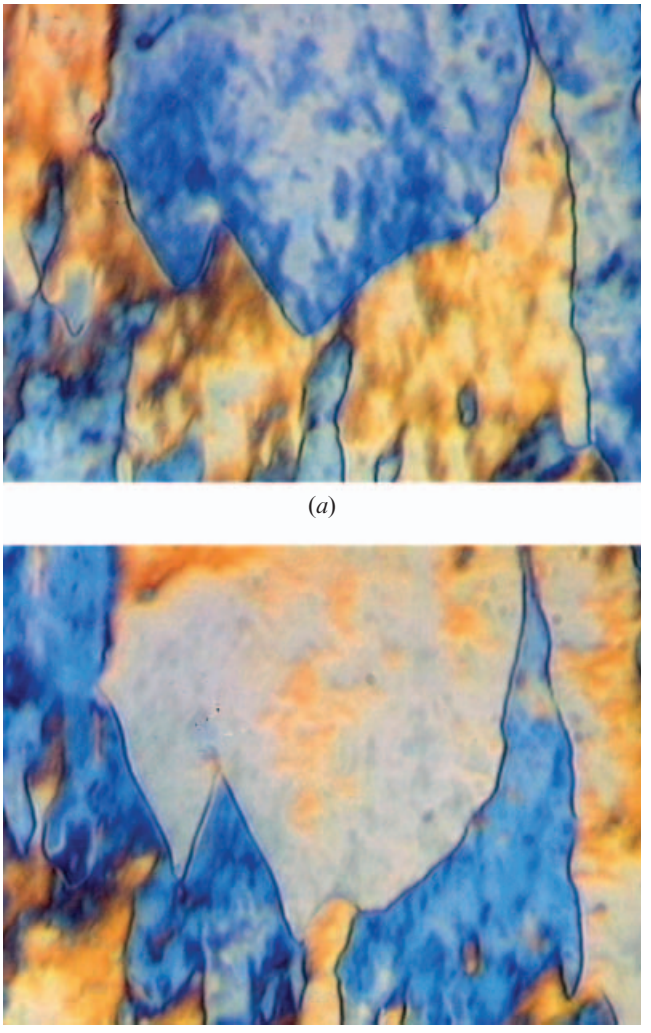

(*a*)

(*b*)

Figure 13. Texture of the nematic phase of compound **9Br** observed by rotating one polarizer by 10° (*a*) clock-wise and (*b*) anticlock-wise from the crossed polarizer position, indicating domains of opposite handedness.

Cl-substituted compounds. The homologues **5Br**, **6Br** and **7Br** form a mesophase which displays a SmA-like fan-shaped texture on slow cooling of the isotropic liquid or the nematic phase, see figure 16 (*a*). This phase shows no homeotropic texture, but a schlieren texture instead, indicating a biaxial structure. For compound **5Br** the layer spacing d of the smectic phase was found to be 1.94 nm which is clearly smaller than the half length of the bent molecule ($L = 4.5$ nm). This result points to a B_6 phase in which the bent molecules are intercalated and, in addition, tilted with respect to the layer normal [10, 11]. In contrast to the B_6 phase described in earlier papers, however, we found an electro-optical response. Above an electric field of $1.5\,V\,\mu m^{-1}$ the red coloured fan-shaped texture

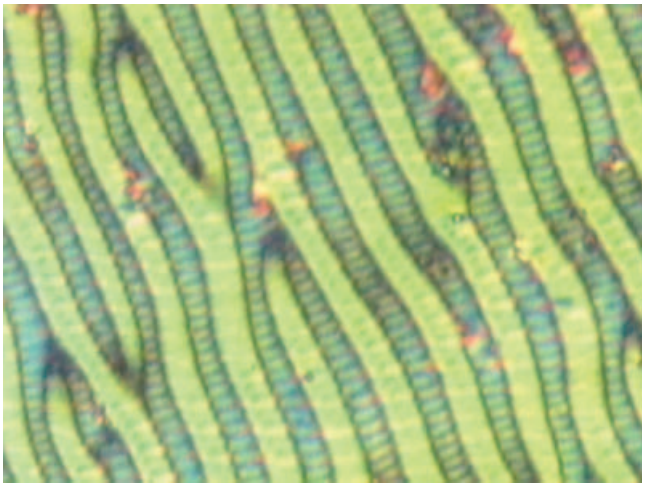

Figure 14. Field-induced domains perpendicular to the original director direction in the nematic phase of compound **12Br** (sample thickness 10 µm, voltage 30 V, 50 Hz, temperature 88°C).

becomes green, figure 16 (*b*); the textures of the switched states are independent of the polarity of the field. Since this effect is also observed at high frequencies (≈10 kHz) it can be assumed that this switching corresponds to a dielectric reorientation, but the mechanism is not yet clear.

Compound **5′Br**, which possesses terminal pentyl chains, forms a monotropic nematic phase. On fast cooling the nematic phase is transformed into a mosaic texture at 63°C. An assignment of this low temperature phase was impossible because this phase crystallizes immediately after its formation from the nematic phase. The nucleation of the mosaic texture and also the relatively high viscosity point to a columnar phase. The same dimorphism was also observed for the homologue **8Br** (see table 1).

5. Discussion

The results reported in the preceding sections clearly proved that a N phase with chiral domains of opposite

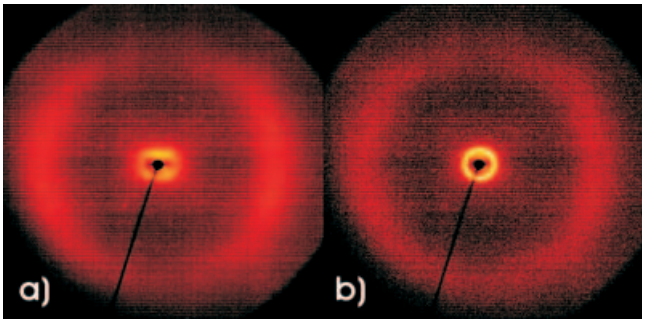

Figure 15. X-ray pattern of (*a*) the nematic phase and (*b*) the X phase of compound **12Br**.

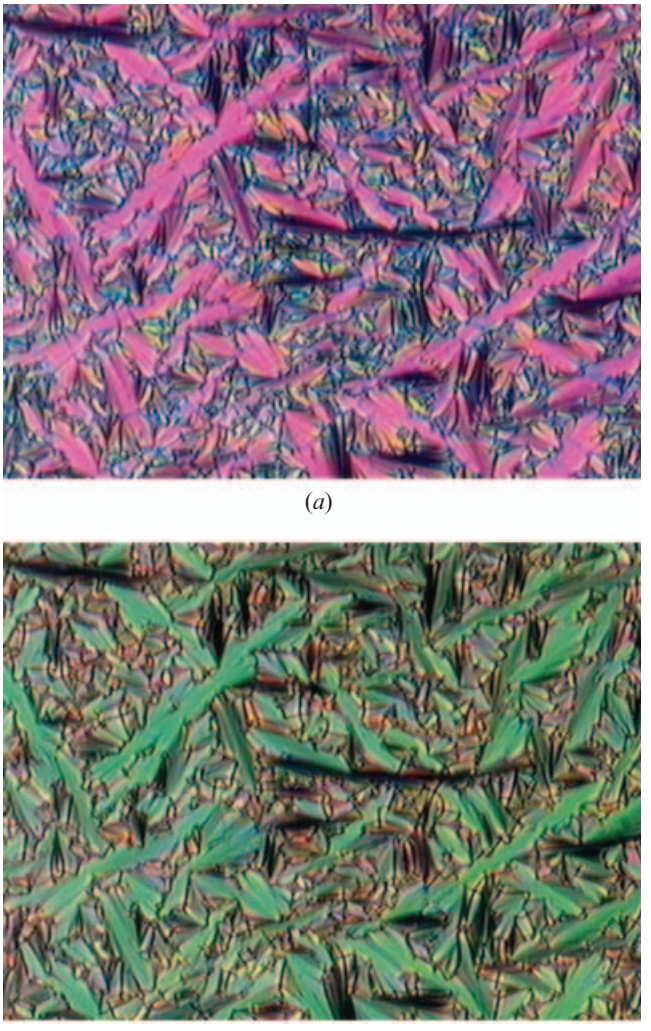

(*a*)

(*b*)

Figure 16. Fan-shaped texture of the B_6 phase of compound **5Br**: (*a*) without electric field and (*b*) + 100V (sample thickness: 6 μm; temperature: 107°C).

handedness exists and that by cooling this phase an isotropic phase appears which also spontaneously forms chiral domains of opposite handedness. It is known that smectic phases of bent-core compounds can exhibit ferroelectric or antiferroelectric properties as a consequence of the sterically induced polar packing [12, 13]. But there are cases in which the bent-core compounds are able to form nematic phases [14–19], sometimes also in combination with 'banana' phases [20, 21]. Within homologous series of bent-core compounds the nematic phase generally arises in members with short terminal chains. It was found that this nematic phase of bent-core compounds shows no significant differences when compared with nematic phases of calamitic compounds. This was surprising since computer simulations [4] as well as theoretical considerations [3] suggest that the bend shape of the molecules can induce a spontaneous local bent of the nematic director giving rise to twist–bend deformations. We were able to observe such deformations in the nematic phase of compound **12Cl** [1]. In addition, a field-induced transition from a planar into a fan-shaped texture was found. In this case the originally partially twisted structure is probably deformed by the external electric field in such a way that a fan-like texture is built up, which is characteristic for a cholesteric phase. It should be noted that bend–twist deformations in the nematic phase of bent-core compounds were also described by Niori *et al*. [22].

The question arises as to why such properties are not observed in nematic phases of other bent-core compounds. It is known that the formation of polar structures (e.g. in SmCP phases) strongly depends on the bending angle, which is the angle between the wings of the bent molecule. On the other hand, the bending angle can be changed by substituents at the central core as well as by flexibility of the linkage groups [10]. In cases where the nematic phase is the high temperature phase with respect to the 'banana' phase, the bending angle significantly decreases with decreasing temperature. There are indications that in the nematic phase of most bent compounds studied the molecules are more or less stretched. In the compounds under investigation, however, the bend angle is pronounced (bending angle $\approx 140^{\circ}$) so that short range polar structures and spontaneous twist deformations are plausible. The possibility of spontaneous twisting is also manifested in the optically isotropic X phase which also forms chiral domains. Since the constituent molecules are achiral it is plausible that domains of opposite handedness occur with equal probability. The origin of the chiral domains is not yet clear. These domains could be caused by molecular chirality as indicated by FTIR spectroscopy [23]. Another reason could be the layer chirality that occurs in 'banana' phases with director tilt and polar order [13].

It follows from our X-ray studies that the FWHM of the small angle reflection in the X phase is clearly smaller than that of the nematic phase which exhibits cybotactic smectic groups. This result indicates that the structure of the X phase is built up by smectic layers. It is also obvious from the X-ray experiments that the alignment is completely lost at the transition from the nematic to X phase. The sequence: oriented sample (N phase) – non-oriented sample (X phase) – oriented sample (crystalline phase) suggests that the random distribution of the layer normals is an intrinsic property of the X phase and not a misalignment. Although the structure of the X phase is isotropic as indicated by

dielectric, NMR and optical measurements, we do not find the typical X-ray pattern of a cubic phase. The reason could be that the lattice parameter of the cubic phase is in the UV range, as in blue phases, preventing detection by the usual X-ray or optical scattering of visible light.

Since X-ray studies suggest the existence of smectic layers the structure could be analogous to the so-called smectic blue phase which exhibits both a three-dimensional orientational order, like the classic blue phases, and smectic positional order [24, 25]. To date smectic blue phases have been found between the isotropic and the TGB phase. The structure can be regarded as the three-dimensional counterpart of the twist grain boundary TGB phase. An essential precondition for the formation of TGB phases or smectic blue phases is the chirality of the molecules. In the compounds under discussion the molecules are achiral. In this case the existence of an isotropic mesophase with chiral domains may be due to the chiral smectic layers which occur because of the combination of polar packing and director tilt [13]. Since the constituent molecules are in chiral smectic layers, macroscopic domains with opposite handedness can obviously be formed with equal probability.

References

[1] Pelzl, G., Eremin, A., Diele, S., Kresse, H., and Weissflog, W., 2002, *J. mater. Chem.*, **12,** 2591.

[2] Eremin, A., Diele, S., Pelzl, G., and Weissflog, W., 2003, *Phys. Rev. E*, **67,** 020 702.

[3] Dozov, I., 2002, *Europhys. Lett.*, **56,** 247.

[4] Memmer, R., 2002, *Liq. Cryst.*, **29,** 483.

[5] Maier, W., and Meier, G., 1961, *Z. Naturforsch.*, **16a,** 262.

[6] Pelzl, G., Diele, S., Grande, S., Jakli, A., Lischka, C., Kresse, H., Schmalfuss, H., Wirth, I., and Weissflog, W., 1999, *Liq. Cryst.*, **26,** 401.

[7] Wirth, I., Diele, S., Eremin, A., Grande, S., Kovalenko, L., Pancenko, N., and Weissflog, W., 2001, *J. mater. Chem.*, **11,** 1642.

[8] Dehne, H., Pötter, H., Sokolowski, S., Weissflog, W., Diele, S., Pelzl, G., Wirth, I., Kresse, H., Schmalfuss, H., and Grande, S., 2001, *Liq. Cryst.*, **28,** 1269.

[9] Diele, S., Grande, S., Kruth, H., Lischka, C., Pelzl, G., Weissflog, W., and Wirth, I., 1998, *Ferroelectrics*, **212,** 169.

[10] Pelzl, G., Diele, S., and Weissflog, 1999, *Adv. Mat.*, **11,** 707.

[11] Weissflog, W., Wirth, I., Diele, S., Pelzl, G., Schmalfuss, H., Schoss, T., and Würflinger, A., 2001, *Liq. Cryst.*, **28,** 1603.

[12] Niori, T., Sekine, T., Watanabe, J., Furukawa, T., and Takezoe, H., 1996, *J. mater. Chem.*, **6,** 213.

[13] Link, D. R., Natale, G., Shao, R., Maclennan, J. E., Clark, N. A., Körblova, E., and Walba, D. M., 1997, *Sience*, **278,** 1924.

[14] Vorländer, D., and Apel, A., 1932, *Ber. Dtsch. Chem. Ges.*, **65,** 1101.

[15] Matzunaki, H., and Matsunaga, Y., 1993, *Liq. Cryst.*, **14,** 105.

[16] Matraszek, J., Mieczkowski, J., Szydlowska, J., and Gorecka, E., 2000, *Liq. Cryst.*, **27,** 429.

[17] Szydlowska, J., Matraszek, J., Mieczkowski, J., Gorecka, E., and Pochiecha, D., 2001, *Mol. Cryst. liq. Cryst.*, **366,** 107.

[18] Stojadinovic, S., Adorjan, A., Sprunt, S., Sawade, H., and Jakli, A., *Phys. Rev. E*, **66,** 060 701(R).

[19] Schröder, M. W., Diele, S., Pelzl, G., Dunemann, U., Kresse, H., and Weissflog, W., 2003, *J. mater. Chem.*, **13,** 1877.

[20] Weissflog, W., Nadasi, H., Dunemann, U., Pelzl, G., Diele, S., Eremin, A., and Kresse, H., 2001, *J. mater. Chem.*, **11,** 2748.

[21] Reddy, A. R., Sadashiva, B. K., and Dhara, S., 2001, *Chem. Commun.*, 1972.

[22] Niori, T., Yamamoto, Y., and Yokohama, H., *Mol. Cryst. liq. Cryst*. (in the press).

[23] Zennyoji, M., Takanishi, Y., Ishikawa, K., Thisayukta, J., Watanabe, J., and Takezoe, H., 2001, *Mol. Cryst. liq. Cryst.*, **366,** 693.

[24] Li, M. H., Laux, V., Nguyen, H. T., Sigaud, G., Barois, P., and Isaert, N., 1997, *Liq. Cryst.*, **23,** 389.

[25] Grelet, E., Collings, P. J., Li, M.-H., Laux, V., and Nguyen, H. T., 2001, *Eur. Phys. J. E*, **6,** 157.